NJC

Accepted Manuscript

This is an *Accepted Manuscript*, which has been through the Royal Society of Chemistry peer review process and has been accepted for publication.

Accepted Manuscripts are published online shortly after acceptance, before technical editing, formatting and proof reading. Using this free service, authors can make their results available to the community, in citable form, before we publish the edited article. We will replace this *Accepted Manuscript* with the edited and formatted *Advance Article* as soon as it is available.

You can find more information about *Accepted Manuscripts* in the Information for Authors.

Please note that technical editing may introduce minor changes to the text and/or graphics, which may alter content. The journal's standard Terms & Conditions and the Ethical guidelines still apply. In no event shall the Royal Society of Chemistry be held responsible for any errors or omissions in this *Accepted Manuscript* or any consequences arising from the use of any information it contains.

ROYAL SOCIETY OF CHEMISTRY

www.rsc.org/njc

Facile Synthesis of Shape-Controlled Graphene/Polyaniline Composites for High Performance Supercapacitor Electrode Materials

Xiaomiao Feng,*[1a] Ningna Chen,[1a] Jinhua Zhou, [a] Yi Li, [a] Zhendong Huang, [a] Lei Zhang, [a] Yanwen Ma,* [a] Lianhui Wang, [a] and Xiaohong Yan [b]

(a) Key Laboratory for Organic Electronics and Information Displays & Institute of Advanced Materials, National Jiangsu Syngerstic Innovation Center for Advanced Materials (SICAM), (b) College of Electronic Science and Engineering, Nanjing University of Posts & Telecommunications, 9 Wenyuan Road, Nanjing 210023, China

* Corresponding authors.

E-mail addresses: iamxmfeng@njupt.edu.cn, iamywma@njupt.edu.cn

[1] These authors contributed equally to this work.

Abstract: Graphene/polyaniline (PANI) nanocomposites with different morphologies were successfully fabricated by an effective one-step hydrothermal method. The morphologies of PANI can be controlled from nanowires to nanocones by adjusting the amount of aniline with the assistance of ultrasonication process. By taking the advantages of the high conductivity of graphene and pseudocapacitance of PANI, the graphene/PANI composites were taken as an example for the application to the supercapacitor eletrode materials. The cyclic voltammograms (CV) and galvanostatic charge/discharge measurements demonstrate that the graphene/PANI shows excellent electrochemical properties. The graphene/PANI nanowire composite (724.6 F/g) exhibited higher specific capacitance than that of the graphene/PANI nanocone composite (602.5 F/g) at a current density of 1.0 A/g. Furthermore, the graphene/PANI nanowire composite exhibits outstanding capacitive performances with a high specific capacitance of 957.1 F/g at 2 mV/s and a high cycle reversibility of 90% after charge/discharge 1000 cycles. The improved electrochemical properties of the graphene/PANI nanocomposites suggest their promising application for high-performance supercapacitors.

1. Introduction

The electrochemical supercapacitors, owing to their high power density, high charge-discharge rate, and long cycling life, are required to address the colossal energy requirements against the backdrop of global warming and the looming energy crisis.[1] In recent years, supercapacitors become the promising energy storage devices and have attracted considerable attention due to their wide applications in many fields, such as electric vehicles, portable electronic devices, memory back-up devices, large industrial equipment, and renewable energy power plan.[2-4] According to the different charge-storage mechanism, they are basically divided into electrochemical double-layer capacitors

(EDLCs) and pseudocapacitors. The former capacitance is arised from the carbon electrodes that store and release energy by charge separation at the interface between electrode and electrolyte. The latter pseudocapacitance including metal oxides and conducting polymers relies on electrosorption and surface redox processes of the electroactive species.[5] Generally, EDLCs can obtain a long electrochemical stability but with relatively low specific capacitance. In contrast, pseudocapacitors can supply a high specific capacitance but with poor cycle life, which limits their real application in supercapacitors. Therefore, the preparation of the supercapacitor electrode materials of carbon nanomaterials and conductive polymers composites with high specific capacitance and long cycle stability by taking the advantages of EDLCs and pseudocapacitors is still kept scientifically challenge.

Carbon nanomaterials, in particular as electrode materials for supercapacitor, have attracted the scientific community in EDLCs due to their large surface areas and good conductivity.[6-8] Among them, graphene, which consists of a sp^2-hybridized carbon atoms packaged into honeycomb lattice structure, offers many outstanding properties, such as high electrical conductivity, high theoretical specific area, superior mechanical properties, as well as low fabrication cost. Hence, graphene is considered as one of the best candidates for electrode materials.[9] It shows good stability during charge-discharge process, but the specific capacitance (around 100 to 200 F/g) is limited by the stores energy mechanism, which mainly relies on the electric double-layer capacitor.[10] On the contrary, as promising electrode materials for pseudocapacitors, conducting polymers can provide high specific capacitance but poor stability, which mainly base on Faradic mechanism.[11] To obtain the perfect performance electrode materials for supercapacitors with high specific capacitance and good stability, much effort has been focused on combining conducting polymers with graphene, such as graphene/polyaniline (PANI),[12-14] graphene/polypyrrole,[15,16] and graphene/polythiophene composites.[17,18] Among these conductive polymers, PANI is especially prominent for promising active electrode materials for the pseudocapacitors, owing to its low cost, easy synthesis, and high theoretical specific pseudocapacitance.[19]

Graphene/PANI has been regarded as one of the most important nanocomposites due to their high theoretical specific pseudocapacitance according to the multiple redox states of PANI.[20,21] The combination of graphene and PANI takes advantage of them to provide a superior performance in supercapacitors.[22] For instance, our group has reported one-step electrochemical synthesis of graphene/PANI composite film with a high capacitance of 640 F/g at 0.1 A/g.[23] Wu et al. obtained a

graphene/PANI nanofiber by vacuum filtration with calculated capacitance of 210 F/g at 0.3 A/g and 194 F/g at 3 A/g, respectively.[24] Zhang et al. demonstrated on a PANI-doped graphene composite by in situ polymerization of aniline monomer in the presence of graphene oxide under acid conditions, which presented capacitance of 480 F/g at 0.1 A/g.[22] Xu et al. discussed the hierarchical graphene/PANI nanowires composites by dilute polymerization that can reach as high as 555 F/g at 0.2 A/g, while the randomly connected PANI nanowires only have 298 F/g under the same condition.[25] However, there are few reports about shape-controlled graphene/PANI nanocomposites preparing by using one-step hydrothermal method.

Herein, a facile one-step hydrothermal method was proposed to synthesize graphene/PANI nanocomposites with different shapes. The morphologies of PANI can be effectively controlled from nanowires to nanocones by adjusting the amount of aniline with the assistance of ultrasonication process. The morphology and structure was characterized by SEM, FT-IR, UV-vis, and XPS. Besides, the electrochemical performance of graphene/PANI composites as supercapacitor electrode materials was explored by cyclic voltammograms (CV) and galvanostatic charge/discharge. The graphene/PANI nanowire composite exhibited the preeminent capacitive performance with a high specific capacitance of 957.1 F/g at a scan rate of 2 mV/s and a high cycle reversibility of 90% after charge/discharge 1000 cycles at a current density of 1.0 A/g. By combination with graphene, the PANI/graphene composites have been endowed excellent performances as supercapacitor electrode materials by harnessing the high conductivity of graphene and pseudocapacitance of PANI.[26] This method might be used to synthesize other graphene/conducting ploymer nanocomposites for high performance supercapacitor electrode materials.

2. Experimental section

2.1 Materials

Graphite flake (natural, -325 mesh, 99.8%) was purchased from Alfa Aesar Chemical Reagent Co. to be used for synthesis of graphene oxide (GO). GO was synthesized by the modified Hummers method as described previously.[23] Aniline monomer, ammonium persulfate (APS), H_2SO_4 (98%), acetylene black, polytetrafluorene ethylene (PTFE), and ethanol were purchased from Shanghai Chemical Reagent Co. Aniline was distilled under reduced pressure and other reagents were used as received without further treatment.

2.2 Preparation of graphene/PANI (nanowires) and graphene/PANI (nanocones) composites

For preparing graphene/PANI nanocomposites, 20 mg of GO was dissolved in 10 mL of 1.0 M H_2SO_4 under magnetic stirring for 1 h. Then 184 μL of aniline monomer was added into the above solution drop by drop and stirring for another 1 h. Subsequently, the APS (1.84 mmol) solution was added into the above solution, which dissolved in 5 mL of 1.0 M H_2SO_4. After that, the mixture was transferred into a Teflon-lined stainless steel autoclave and maintained at a temperature of 140 □ for 12 h. The resulting suspension was separated by centrifugation and washed with deionzed water and ethanol. Afterwards, the mixture was dried at 60 □ under a vacuum for 12 h. Finally, the graphene/PANI nanowire was obtained (abbreviated as GPW-1). The content of aniline monomer was decreased to half of the original amount and the other experimental conditions were same with the above procedure, the graphene/PANI composite with few nanowires was produced (referred to as GPW-2). For obtaining graphene/PANI composites with different shapes, the GO suspension was treated by sonication for 1h before hydrothermal treatment and other experimental conditions were same with the procedure of GPW-1, and then the graphene/PANI nanocones was obtained (named as GPC-1). When the amount of aniline was decreased to half of the original content and other experimental conditions were same with the above procedure of GPC-1, the graphene/PANI with small nanocones was collected (donated as GPC-2).

2.3 Preparation of the graphene/PANI (nanowires) and graphene/PANI (nanocones) composites modified electrodes

To test the electrochemical properties of graphene/PANI composites, a three-electrode cell was assembled. The GPW-1 modified electrode was prepared by mixing 70 wt. % of GPW-1, 25 wt. % of acetylene black, 5 wt. % of PTFE, and a few drops of ethanol. Then the slurry were pressed onto graphite electrodes acting as working electrodes and dried in vacuum at 80 $^{\circ}$C for 12 h before using. The GPW-2, GPC-1, and GPC-2 modified electrodes were also prepared according to the same course. The mass loading of active materials in the electrode was about 9 $mg \cdot cm^{-2}$ and the size of the working electrode was 1 cm^2. In addition, saturated calomel and platinum wire electrodes were used as the reference and counter electrodes, respectively. An aqueous solution of 1.0 M H_2SO_4 was acted as the electrolyte.

2.4 Characterization

The morphologies of the graphene/PANI composites were characterized by scanning electron microscopy (SEM, S4800). Fourier-transform infrared (FT-IR) spectroscopy spectra of products in

KBr pellets were examined using a Bruker model VECTOR22 Fourier transform spectrometer. Ultraviolet-visible (UV-vis) absorption spectra were recorded on a UV-2401PC spectrometer. X-ray photoelectron spectroscopic (XPS) measurements were preceded on ESCA-LAB MK II X-ray photoelectron spectrometer. To estimate the electrochemical properties of the samples, a classical three-electrode fabrication was carried on a CHI 660C electrochemical workstation (Chenhua, Shanghai). The electrochemical behaviors of the supercapacitor systems were recorded by cyclic voltammograms (CV) and galvanostatic charge/discharge measurement. All the amperometric experiments were manipulated with the potential windows of -0.2 to 0.8 V (vs SCE) in a 1.0 M H_2SO_4 electrolyte, where the composite modified graphite electrode was used as the working electrode, a platinum wire as the auxiliary electrode, and a saturated calomel electrode (SCE) as the reference electrode. The specific capacitance could be calculated from the cyclic voltammograms (CV) curves according to equation 1[27, 28]:

$$Cg = (\int IdV) \Big/ (mVv) \quad (1)$$

Where I represent the response current (A), V is the potential window (V), υ is the potential scan rate (mV/s), and m is the mass of the active material in the electrode (g). The specific capacitance was calculated from the galvanostatic charge/discharge curves using eq 2[27]:

$$Cm = I\Delta t \Big/ m\Delta V \quad (2)$$

Where I represent the discharge current (A), Δt is the discharge time (s), m is the mass of the active material in the electrode (g), and ΔV is the potential window (V).

3. Results and Discussion

The graphene/PANI nanocomposites were successfully synthesized by using GO and aniline monomer as starting materials through an easy one-step hydrothermal method. The shape of the composites can be controlled by the amount of aniline monomer and the process of ultrosonication. First of all, GO, which prepared by the modified Hummers method, could be easily dispersed in H_2SO_4 aqueous solution for the existence of many oxygen-containing functional groups on the surface of GO. This may provide and act as the active nucleation sites for anchoring PANI nanostructures.[29] When aniline monomer was dropped into the stable suspension, owing to the strong electrostatic interactions between amino group and oxygen functionalities (-OH, C-O-C on the plane and -COOH) of GO, aniline would be anchored on the surface of GO. It could be

explained that aniline monomer was dispersed in acid solution to form aniline salt and carried positive charge to absorb on the negatively charged surface of GO.[30] Therefore, a homogeneous mixture of GO/aniline suspension could be easily obtained. There are enough aniline monomer absorbed on the GO surface. During hydrothermal procedure, the adsorbed aniline monomers would be oxidized and polymerized to form PANI nanowires along the surface of GO. Meanwhile, GO was reduced to graphene resulting in the formation of the graphene/PANI nanowires. As the aniline monomer content decreased, down to 50 wt % of the original amount and other experimental conditions were same with the above procedure, the graphene/PANI with few and thin nanowires was obtained. However, when the GO solution was experienced one hour ultrasonication at the initial step, the graphene/PANI nanocones were observed. The possible reason may be that the GO is partly reduced under ultrasonication in acid solution and supply limited active sites for absorbance of aniline. The limited active sites cannot make aniline monomer polymerize on the surface of GO effectively. Therefore, parts of aniline will be grown overhead GO to form PANI nanocones. Similarly, the nanocones structure became small and short when the amount of aniline monomer was reduced. Compared with those reported works[25, 27, 31], most of their preparation methods were relatively complex and the shapes of resulting products were single. In this work, the morphologies of PANI on the surface of graphene could be easily controlled from nanowires to nanocones by adjusting the amount of aniline without any surfactants that was rarely reported.

Fig. 1A and 1B show the SEM images of GPW-1 with different magnifications, where we can see the PANI nanowires with an average diameter about 140 nm and length of 1-3 μm that densely grow on the surface of graphene. Due to the reduced amount of the aniline, the sparse PANI nanowires with decreased sizes in diameter about 100 nm and length of 1-2 μm of GPW-2 uniformly distributed on the surface of graphene, as shown in Fig. 1C and 1D. When the GO aqueous suspension was treated by ultrasonication, the PANI nanocones could be obtained, as shown in Fig. 1E and 1F. When the amount of aniline monomer was reduced, nanocones became smaller as revealed in Fig. 1G and 1H. The tremendous changes of morphology revealed that the amount of aniline play an important role in the shape, which might affect the electrochemical performances greatly.[32] Another reason might be ascribed to the role of ultrasonication, which facilitated the mechanical exfoliation and simultaneously partial reduction of GO leading to that it became hydrophobic and supplied the limited the reactive sites.[33] Besides, graphene/PANI composites experienced a long sonication step during the preparation of the SEM specimen,

implying the strong electrostatic interaction between graphene and PANI.[24] This may be favorable for the enhancement of the electrochemical performances as electrode materials for supercapacitors.[34]

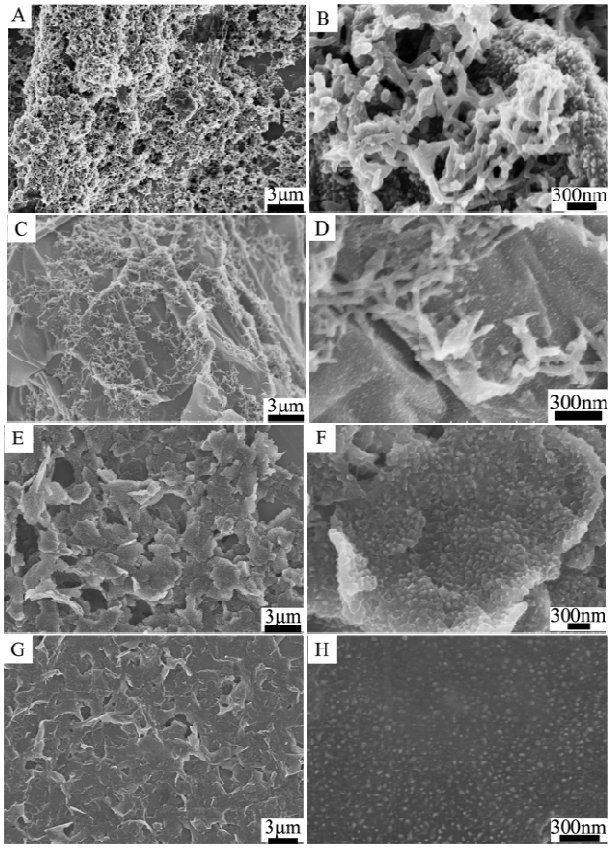

Fig. 1 SEM images with different magnifications of GPW-1(A and B), GPW-2(C and D), GPC-1(E and F), and GPC-2(G and H).

The composites structures were further proved by UV-vis spectra. In general, the UV-vis spectra of graphene/PANI nanocomposites exhibited three absorption peaks at 349, 440, and 824 nm with a free tail extended to the IR region, respectively. They were attributed to the absorption of PANI and could be assigned to polaron-π*, π-π* transition, and π-polaron transitions, respectively.[23] However, the absorption peaks of the π-polaron transition of GPW-1 and GPC-1 were stronger and shifted to higher wavelength than that of GPW-2 and GPC-2 indicating that the PANI of GPW-1 and GPC-1 with higher doping level was more delocalized, which would be beneficial to the supercapacitor properties.[32]

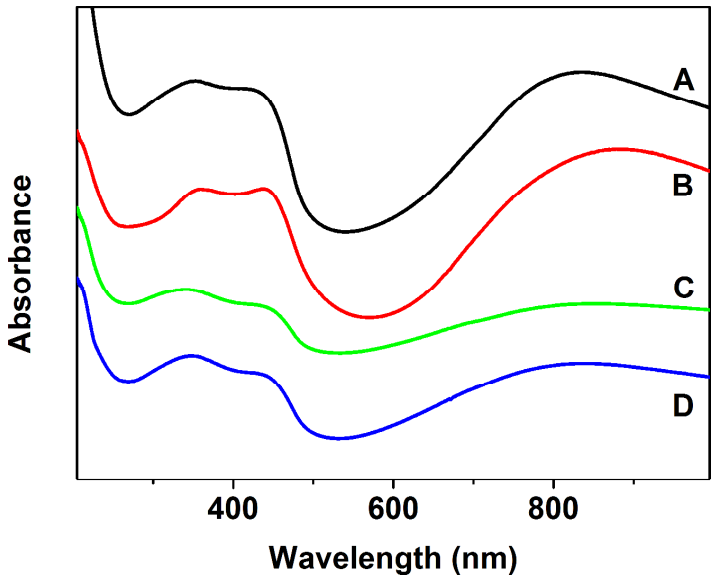

Fig. 2 UV-vis spectra of GPW-1(A), GPC-1(B), GPW-2(C), and GPC-2(D).

FT-IR was employed to investigate the structures of the nanocomposites. In the FT-IR spectrum of GO (Fig. 3A), the peaks around 3427, 1730, 1628, 1406, and 1052 cm^{-1} were attributed to the characteristic vibrations of the hydroxyl group, C=O in COOH, intercalated water, and C-O in C-OH/C-O-C functional groups, respectively.[35] It also showed an absorption peak at 1227 cm^{-1} due to the stretching vibration of epoxy C-O group. After the hydrothermal process, the GO was reduced to graphene and most of the oxygen-containing functional groups had been removed by the hydrothermal reduction. In the spectra of composites (Fig. 3B, C, D, and E), the bands at 1570 and 1483 cm^{-1} were assigned to C=C stretching vibrations of quinoid and benzenoid rings of PANI, respectively. The peaks at 1298 and 1236 cm^{-1} were related to the C-N and C=N stretching modes. The in-plane bending of C-H was reflected in the 1131 cm^{-1}. The peak at 815 cm^{-1} was attributed to the out-of-plane bending of C-H. In addition, the peak at 3445 cm^{-1} was ascribed to O-H in molecular of water. These characteristic peaks were in agreement with the FT-IR features of pure PANI, which demonstrated the presence of PANI was existent in the composites.[36]

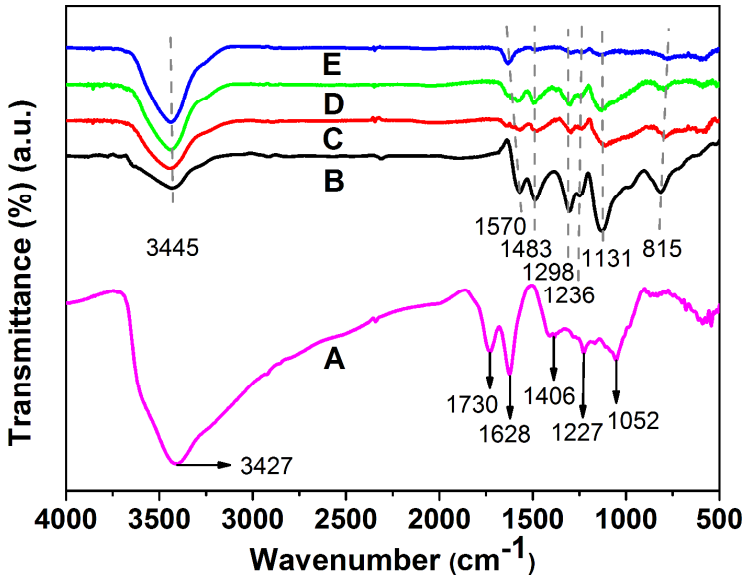

Fig. 3 FTIR spectra of GO (A), GPW-1(B), GPC-1(C), GPW-2(D), and GPC-2(E).

The composition of the graphene/PANI nanocomposites was analyzed by XPS. The wide scan spectra and high resolution C (1s) and N (1s) spectra of GO (a), GPW-1(b), and GPC-1(c) were shown in Fig. 4. Compared with the spectrum of GO, two new elementals (S and N) were observed in the wide scan spectrum of graphene/PANI composites, indicating the presence of PANI, which doped by SO_4^{2-}.[23] The curve fitting of C 1s spectrum of GO core-level which was fitted by XPSPEAK41 program (both Gaussian and Lorizon) could be reasonably decomposed into four peaks with binding energies of 284.7 (C-C), 286.6 (C-O), 287.2 (C=O), and 288.5 eV (O=C-OH), as shown in Fig. 4Ba.[6] Besides the four Gaussian peaks, a new peak around 285.0 eV attributed to C-N was observed in the graphene/PANI composites corresponding to the structure of PANI as revealed in Fig. 4Bb and 4Bc.[23] Compared to GO spectrum, the oxygen content in the composites were significantly decreased. The reduced oxygen-containing functional groups increases the sp^2 carbon content of graphene, resulting in enhance of the π-π interaction between graphene and PANI, which may promote the electron transfer and produce a synergies on electrochemical properties of the composites.[34] N 1s XPS spectra of GPW-1 and GPC-1 were given in Fig. 4(C). The high-resolution XPS of the N 1s region of hybrids could be fitted by three different electronic states, the benzenoid amine at 398.4 eV (=N-), the quinoid amine at 399.1 eV (-NH-), and the nitrogen cationic radical at 401.1 eV ($N^{+\cdot}$), respectively. The XPS results, together with the UV-vis absorption spectra, indicating that PANI structure in the composites was in doped state.

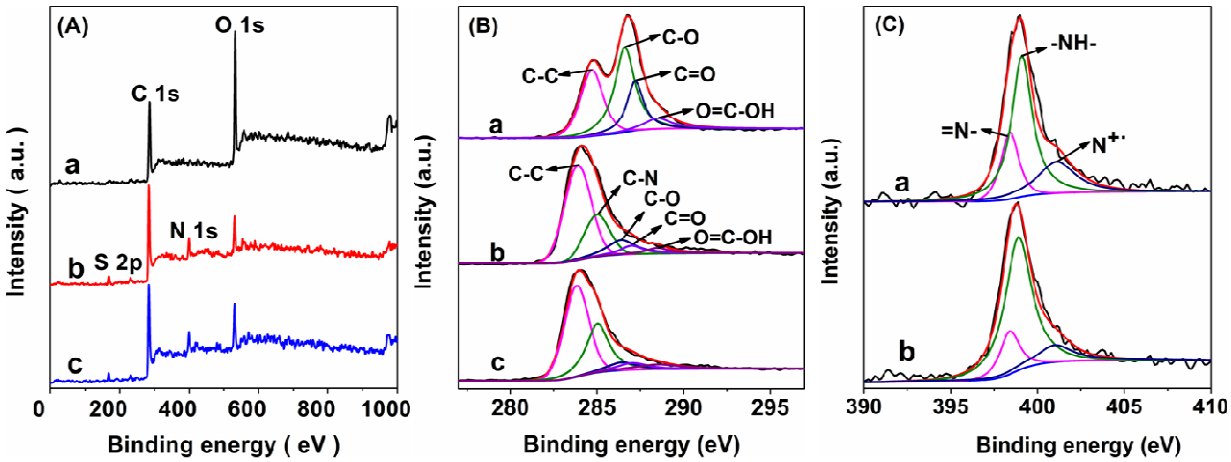

Fig. 4(A) XPS spectra of GO (a), GPW-1(b), and GPC-1(c); (B) XPS data of the C1s regions of GO (a), GPW-1(b), and GPC-1(c); (C) XPS data of the N1s regions of GPW-1(a) and GPC-1(b).

The electrochemical performance of GPW-1, GPC-1, GPW-2, and GPC-2 was evaluated by cyclic voltammetry (CV) and galvanostatic charge/discharge in 1.0 M H_2SO_4 electrolyte at a potential window from -0.2 to 0.8 V. All electrochemical tests of supercapacitors were based on three-electrode system. Fig. 5(A) illustrated the CVs of GPW-1(a), GPC-1(b), GPW-2(c), and GPC-2(d) at a scan rate of 100 mV/s. Generally, two pairs of redox peaks appeared in all of graphene/PANI composites, which were attributed to two redox transitions of PANI (i.e., the leucoemeraldine-emeraldine transition and the emeraldine-pernigraniline transition).[25] Among the enclosed areas of the CV curves of GPW-1(Fig. 5Aa), GPC-1(Fig. 5Ab), GPW-2(Fig. 5Ac), and GPC-2(Fig. 5Ad), the area of GPW-1 CV curve was the largest. The specific capacitance of GPW-1 could reach 540 F/g at this condition. Under the identical measurements, the specific capacitance of GPC-1, GPW-2, and GPC-2 was 429.4, 406.6, and 344.4 F/g, respectively. As it can be seen, with the amount of aniline monomer is reduced, the capacitance value will be decreased. From the above results, GPW-1 had better capacitive properties than those of others, which was also confirmed by the charge-discharge experiments. Fig. 5(B) presented the galvanostatic charge/discharge curves of the supercapacitors based on graphene/PANI composites at a current density of 1.0 A/g. As shown in Fig.5 (B), the discharge curve of graphene/PANI composites consists of two different curvatures in the total range of potential, showing the combination of double-layer capacitive behavior and pseudocapacitance performance in the composites.[37] The initial straight linear section corresponds to the fast discharge of the electric double layer and the latter nonlinear part comes from the pseudocapacitantive behavior.[16] In addition, the IR drops on all the curves were not obvious,

indicating that the resistance was very small and there was good contact between the electrode material and the collectors. The specific capacitances were 593.4, 446.1, 411.9, and 394.9 F/g of GPW-1, GPC-1, GPW-2, and GPC-2, respectively. The large specific capacitance of the composites might be due to the high conductivity of graphene and pseudocapacitance of PANI. From the results of CV and galvanostatic charge/discharge, we could see GPW-1 exhibited the best capacitive performance among these composites. In the following studies, GPW-1 was taken as an example for the study of the application in supercapacitor electrode materials.

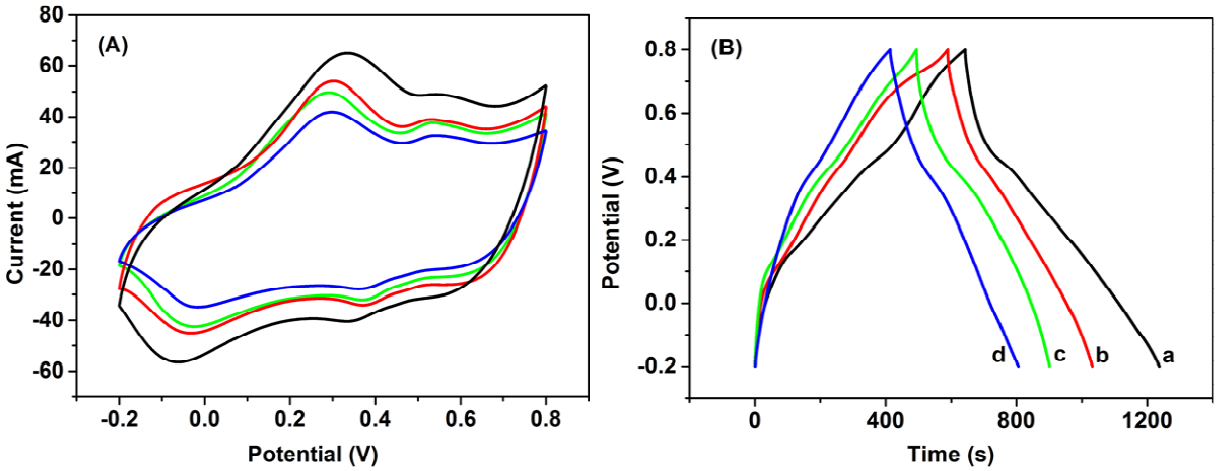

Fig. 5 (A) Cyclic voltammograms of GPW-1(a), GPC-1(b), GPW-2(c), and GPC-2(d) at 100 mV/s scan rate; (B) Galvanostatic charge/discharge curves of the GPW-1(a), GPC-1(b), GPW-2(c), and GPC-2(d) at current density of 1.0 A/g with potential windows of -0.2 to 0.8 V in 1 M H_2SO_4.

Fig. 6(A) displays CV curves of GPW-1 at different scan rates of 2, 5, 10, 25, 50, 75, 100, 200, 300, 400, and 500 mV/s in 1.0 M H_2SO_4 aqueous solution with potential window from -0.2 to 0.8 V. Two couples of redox peaks were observed in the CV curves. It is well-known, PANI exists in three well-defined oxidation states: leucoemeraldine, emeraldine, and pernigraniline. The amine/imine ratio is different in the different states of PANI. The first and second oxidation waves correspond to the transition of leucoemeraldine to emeraldine salt and emeraldine salt to pernigraniline state in acid media, respectively.[38] Furthermore, the CV curves with considerably high redox current and capacity exhibited rectangle-like shapes, which indicated the supercapacitor had large double-layer capacitance and pseudocapacitance. However, the symmetrical CV curves were distorted with the increase of scan rates, which was assigned to the combined double-layer and pseudocapacitive contributions to the total capacitance.[39] The specific capacitance of GPW-1 as a function of scan rates was displayed in Fig. 6(B). The calculated specific capacitance values of GPW-1 at 2, 5, 10, 25,

50, 75, 100, 200, 300, 400, and 500 mV/s were 957.1, 805.7, 742.9, 677.1, 620, 578.7, 540, 441.1, 382.1, 322, and 279.7 F/g, respectively. Due to the unique structural characteristics and synergistic effect between graphene and PANI, the high specific capacitance was obtained. With the increase of the scan rate, the electrolyte ion could not contact with the surface and internal of active electrode fully leading to the decrease of the specific capacitance. Therefore, the capacitance of graphene/PANI not only comes from Faradic reactions of PANI at the electrode/electrolyte surface, but also from that of the electric double-layer capacitance of carbon-based materials.[25]

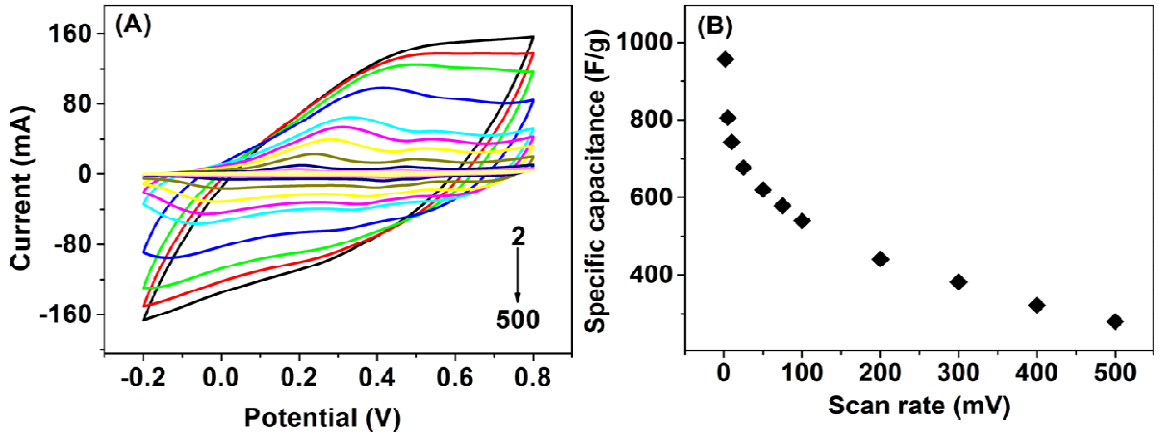

Fig. 6(A) Cyclic voltammograms of GPW-1 at different scan rates from inner to outside (2, 5, 10, 25, 50, 75, 100, 200, 300, 400, and 500 mV/s), respectively; (B) Specific capacitance of GPW-1 at different scan rates as a function of scan rate.

To evaluate the electrochemical performance about GPW-1 as electrode material for supercapacitor, galvanostatic charge/discharge measurements were used. Fig. 7(A) demonstrated the galvanostatic charge/discharge curves of the supercapacitors based on the GPW-1 at various charging/discharging current densities from 0.1 to 5.0 A/g. It could be seen from Fig. 7(A), the charge-discharge curves of GPW-1 almost maintain the same shape in the potential range from -0.2 to 0.8 V in 1.0 M H_2SO_4 at different current densities of 0.1, 0.5, 1.0, 2.0, 3.0, 4.0, and 5.0 A/g, which revealed the hybrid material could experience a broad electric current range.[28] Obviously, the discharge curves were not straight lines, suggesting that the capacitance includes not only EDLC but also faradic capacitance. The corresponding specific capacitance of GPW-1 composite was 827.6, 653.5, 593.4, 541.2, 517.5, 504.7, and 493.5 F/g at different current densities of 0.1, 0.5, 1.0, 2.0, 3.0, 4.0, and 5.0 A/g, respectively, shown in Fig. 7(B). The specific capacitance decreases with the charge/discharge current density increases. Generally, the electrolyte ions could not enter into the internal structure of

the electro-active material at higher current density. In addition, the conducting graphene greatly facilitated electron transfer during the charging-discharging process. The synergistic effect, involving the excellent electrical conductivity of graphene and the high pseudocapacitance of the PANI nanostructure, was also beneficial to improve the capacitance properties.

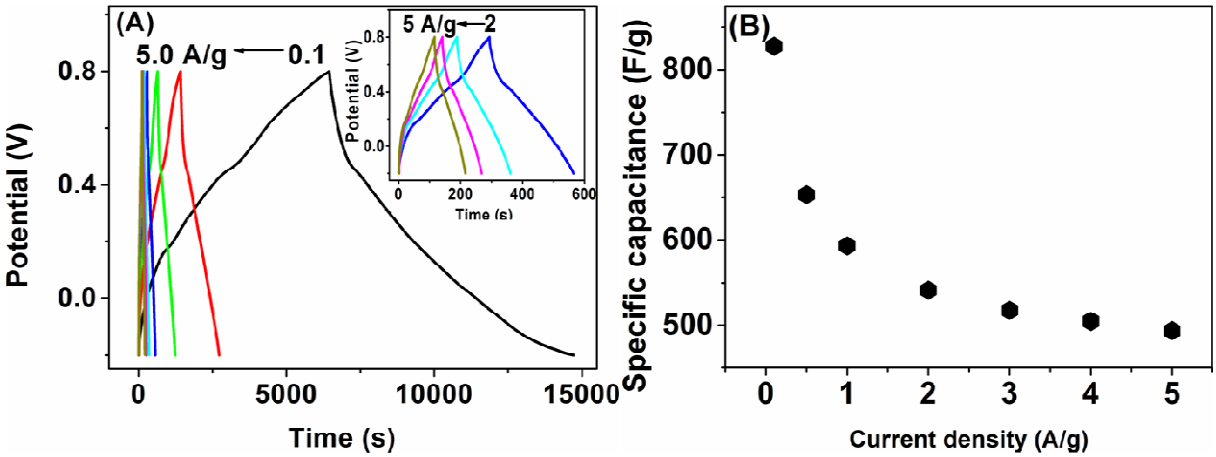

Fig. 7 Galvanostatic charge/discharge (A) and Specific capacitance (B) of GPW-1 in 1.0 M H_2SO_4 at different current densities of 0.1, 0.5, 1.0, 2.0, 3.0, 4.0, and 5.0 A/g, respectively.

The stability of the supercapacitor based on GPW-1 composite during long-term charge/discharge cycling is one of the most significant factors for its practical applications. The long cycle life of the GPW-1 in 1.0 M H_2SO_4 electrolyte solution was tested by galvanostatic charge-discharge at 1.0 A/g over the potential window of -0.2 to 0.8 V, as shown in Fig. 8. The supercapacitor maintained its 90% capacitance (533.6 F/g) of the original value after 1000 cycles, indicating good capacity retention, which was attributed to the synergistic effect between the graphene and PANI. In general case, conducting polymers such as PANI, often supply limited electrochemical stability during charge-discharge process for the reason of the swelling and shrinking of the polymers may lead to decomposition, which limits their applications. Moreover, the active electrode material dissolving in the electrolyte solution contributes to the main factor for capacitance decrease. Yet, the combination of graphene can improve the cycle stability of the graphene/PANI composites-based supercapacitor greatly.[25,40] In the redox process of PANI nanowires, graphene can avoid undermining the electrode material and provide good stability. Additionally, the vertical and scattered PANI nanowires arrays were facile to strain relaxation, which allowed them to decrease the breaking during the doping/dedoping process of counterions.

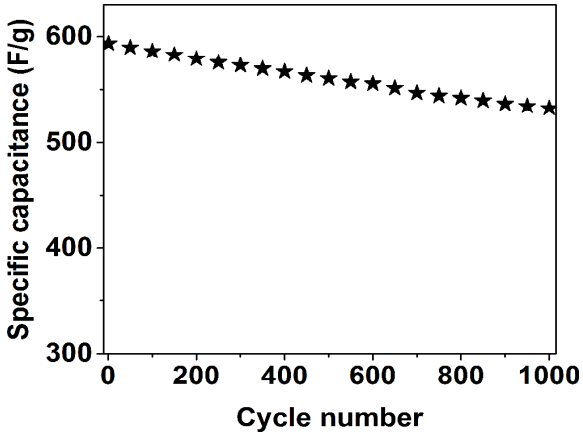

Fig. 8 The specific capacitance changes of GPW-1 at a constant current density of 1.0 A/g as a function of cycle number.

4. Conclusion

In summary, graphene/PANI nanocomposites with different morphologies can be delicately synthesized by hydrothermal method with the assistance of ultrasonication. The morphologies of PANI can be controlled from nanowires to nanocones by adjusting the amount of aniline with the assistance of ultrasonication process. By harnessing the synergistic effect between graphene and PANI, the graphene/PANI nanocomposites can be used as supercapacitor electrode materials. The PANI nanowires and nanocones can facilitate the ion diffusion and improve the utilization of the electroactive PANI resulting in the high performance for supercapacitor. Furthermore, the GPW-1 based supercapacitor has high specific capacitance and good long term stability that after 1000 charging/discharging cycles at a current density of 1.0 A/g. This study may supply a promising and efficient way to obtain excellent electrode materials for energy storage devices with high performance.

Acknowledgment.

We sincerely express our thanks to the '973' (2012CB933301) and '863' projects (2011AA050526), the National Natural Science Foundation of China (Nos. 20905038, 20903057, and 61205195), and the Natural Science Foundation of Jiangsu (BK20141424), and Foundation of Nanjing University of Posts & Telecommunications (NY213172), and the Priority Academic Program Development of Jiangsu Higher Education Institutions (PAPD), and the Ministry of Education of China (IRT1148).

References

1 Y.-N. Meng, K. Wang, Y.-J. Zhang, and Z.-X. Wei, *Adv. Mater.*, 2013, **25**, 6985-6990.

2 S. Patrice and Y. Gogotsi, *Nat. Mater.*, 2008, **7**, 845-854.

3 J.-T. Zhang and X. S. Zhao, *Chemsuschem*, 2012, **5**, 818-841.

4 L.-L. Zhang and X.-S. Zhao, *Chem. Soc. Rev.*, 2009, **38**, 2520 - 2531.

5 Y. Jang, J. Jo, Y.-M. Choi, I. Kim, S.-H. Lee, D. Kim, and S.-M. Yoon, *Electrochim Acta*, 2013, **102**, 240-245.

6 X.-M. Feng, N.-N. Chen, Y. Zhang, Z.-Z. Yan, X.-F. Liu, Y.-W. Ma, Q.-M. Shen, L.-H. Wang, and W. Huang, *J. Mater. Chem. A*, 2014, **2**, 9178-9184.

7 J. -L. Liu, J. Sun, and L. Gao, *J. Phys. Chem. C,* 2010, **114**, 19614-19620

8 J. -L. Liu, J. Sun, and L. Gao, *Nanoscale,* 2011, **3**, 3616-3619.

9 Y.-Q. Sun, Q. Wu, and G.-Q. Shi, *Energy Environ. Sci.* 2011, **4**, 1113-1132.

10 F. Liu, S.-Y. Song, D.-F. Xue, and H.-J. Zhang, *Adv. Mater.*, 2012, **24**, 1089 - 1094.

11 C. Liu , F. Li , L.-P. Ma , and H.-M. Cheng , *Adv. Mater.*, 2010, **22**, E28 - 62.

12 L. Wang, Y.-J. Ye, X.-Q. Lu, Z.-B. Wen, Z. Li, H.-Q. Hou, and Y.-H. Song, *Sci. Rep.*, 2013, **3**, 3568.

13 R.-R. Salunkhe, S.-H. Hsu, K.-C. Wu, and Y. Yamauchi, *ChemSusChem*, 2014, DOI: 10.1002/cssc.201400147.

14 Z.-F. Li, H.-Y. Zhang, Q. Liu, L.-L. Sun, L. Stanciu, and J. Xie, *ACS Appl Mater Inter*, 2013, **5**, 2685-2691.

15 L.-Y. Li, K.-Q. Xia, L. Li, S.-M. Shang, Q.-Z. Guo, and G.-P. Yan, *J Nanopart Res*, 2012, **14**, 908.

16 X.-M. Feng, R.-M. Li, Z.-Z. Yan, X.-F. Liu, R.-F. Chen, Y.-W. Ma, X.-A. Li, Q.-L.Fan, and W. Huang, *Ieee T Nanotech*, 2012, **11**, 1080-1086.

17 F. Alvi, P.-A. Basnayaka, M.-K. Ram, H. Gomez, E. Stefanako, Y. Goswami, and A. Kumar, *J. New Mater. Electrochem. Syst.*, 2012, **15**, 89-95.

18 A. Takahashi, C.-J. Lin, K. Ohshimizu, T. Higashihara, W.-C. Chen, and M. Ueda, *Polymer. Chem.*, 2012, **3**, 479-485.

19 D.-D. Xu, Q. Xu, K.-X. Wang, J. Chen, and Z.-M. Chen, *ACS Appl. Mat. Interfaces.*, 2014, **6**, 200-209.

20 C.-N.-R. Rao, A.-K. Sood, K. S.Subrahmanyam, and A. Govindaraj, *Angew. Chem., Int. Ed.*

2009, **48**, 7752-7777.

21 M. Fang, K.-G. Wang, H.-B. Lu, Y.-L.Yang, and S. Nutt, *J. Mater. Chem.*, 2009, **19**, 7098-7105.

22 K. Zhang, L.-L. Zhang, X.-S. Zhao, and J. Wu, *Chem.Mater.*, 2010, **22**, 1392-1401.

23 X.-M. Feng, R.-M. Li, Y.-W. Ma, R.-F. Chen, N.-E. Shi, Q.-L. Fan, and W. Huang, *Adv. Funct. Mater.*, 2011, **21**, 2989-2996.

24 Q. Wu, Y.-X. Xu, Z.-Y. Yao, A.-R. Liu, and G.-Q. Shi, *ACS Nano.*, 2010, **4**, 1963-1970.

25 J.-J. Xu, K. Wang, S.-Z. Zu, B.-H. Han, and Z.-X. Wei, *ACS Nano.*, 2010, **4**, 5019-5026.

26 N.-A. Kumar and J.-B. Baek, *Chem. Commun.*, 2014, **50**, 6298-6308.

27 L.-F. Lai, H.-P. Yang, L. Wang, B.-K. Teh, J.-Q. Zhong, H. Chou, L.-W. Chen, W. Chen, Z.-X. Shen, R.-S. Ruoff, and J.-Y. Lin, *ACS Nano. ,* 2012, **6**, 5941-5951.

28 J.-Y. Zhu and J.-H. He, *ACS Appl. Mat. Interfaces.*, 2012, **4**, 1770-1776.

29 A.-B. Bourlinos, T.-A. Steriotis, M. Karakassides, Y. Sanakis, V. Tzitzios, C. Trapalis, E. Kouvelos, and A. Stubos, *Carbon*, 2007, **45**, 852-857.

30 D. Li and R.-B. Kaner, *Chem. Commun.*, 2005, **26**, 3286-3288.

31 M.-M. Sk, C.-Y. Yue, and R.-K. Jena, *Polymer*, 2013, **55**, 798-805.

32 H.-L. Wang, Q.-L. Hao, X.-J. Yang, L.-D. Lu, and X. Wang, *ACS Appl. Mat. Interfaces.* , 2010, **2**, 821-828.

33 K. Krishnamoorthy, G. S. Kim, and S. J. Kim, *Ultrason Sonochem*, 2013, **20**, 644-649.

34 H.-L. Wang, Q.-L. Hao, X.-J. Yang, L.-D. Lu, and X. Wang, *Nanoscale.*, 2010, **2**, 2164-2170.

35 S. Park, K.-S. Lee, G. Bozoklu, W. -W. Cai, S.-T. Nguyen, and R.-S. Ruoff, *ACS Nano. ,* 2008, **2**, 572-578.

36 X.-M. Feng, C.-J. Mao, G. Yang, W.-H. Hou, and J.-J. Zhu, *Langmuir. ,* 2006, **22**, 4384-4389.

37 S. Chen, J. Zhu, X. Wu, Q. Han, and X. Wang, *Acs Nano*, 2010, **4**, 2822-2830.

38 Z.-Q. Peng, L.-M. Guo, Z.-H. Zhang, B. Tesche, T. Wilke, D. Ogermann, S.-H. Hu, and K. Kleinermanns, *Langmuir.,* 2006, **2**, 10915-10918.

39 B. Xu, S.-F. Yue, Z.-Y. Sui, X.-T. Zhang, S.-S. Hou, G.-P. Cao, and Y.-S. Yang, *Energy Environ. Sci.*, 2011, **4**, 2826-2830.

40 F. Yang, M. Xua, S. -J. Bao, H. Wei, and H. Chai, *Electrochim. Acta*, 2014, **137**, 381-387.